Cellular/Molecular

Combinatory Actions of Co-transmitters in Dopaminergic Systems Modulate *Drosophila* Olfactory Memories

Daisuke Yamazaki, Yuko Maeyama, and Tetsuya Tabata
Institute of Quantitative Biosciences, The University of Tokyo, Tokyo, 113-0032, Japan

Dopamine neurons (DANs) are extensively studied in the context of associative learning, in both vertebrates and invertebrates. In the acquisition of male and female *Drosophila* olfactory memory, the PAM cluster of DANs provides the reward signal, and the PPL1 cluster of DANs sends the punishment signal to the Kenyon cells (KCs) of mushroom bodies, the center for memory formation. However, thermo-genetical activation of the PPL1 DANs after memory acquisition impaired aversive memory, and that of the PAM DANs impaired appetitive memory. We demonstrate that the knockdown of glutamate decarboxylase, which catalyzes glutamate conversion to GABA in PAM DANs, potentiated the appetitive memory. In addition, the knockdown of glutamate transporter in PPL1 DANs potentiated aversive memory, suggesting that GABA and glutamate co-transmitters act in an inhibitory manner in olfactory memory formation. We also found that, in γKCs, the Rdl receptor for GABA and the mGluR DmGluRA mediate the inhibition. Although multiple-spaced training is required to form long-term aversive memory, a single cycle of training was sufficient to develop long-term memory when the glutamate transporter was knocked down, in even a single subset of PPL1 DANs. Our results suggest that the mGluR signaling pathway may set a threshold for memory acquisition to allow the organisms' behaviors to adapt to changing physiological conditions and environments.

Key words: **co-transmitters; dopamine; glutamate; metabotropic glutamate receptor; GABA; long-term memory**

Significance Statement

In the acquisition of olfactory memory in *Drosophila*, the PAM cluster of dopamine neurons (DANs) mediates the reward signal, while the PPL1 cluster of DANs conveys the punishment signal to the Kenyon cells of the mushroom bodies, which serve as the center for memory formation. We found that GABA co-transmitters in the PAM DANs and glutamate co-transmitters in the PPL1 DANs inhibit olfactory memory formation. Our findings demonstrate that long-term memory acquisition, which typically necessitates multiple-spaced training sessions to establish aversive memory, can be triggered with a single training cycle in cases where the glutamate co-transmission is inhibited, even within a single subset of PPL1 DANs, suggesting that the glutamate co-transmission may modulate the threshold for memory acquisition.

Introduction

Associative learning, a basic form of memory, is conserved through evolution, and its underlying cellular and molecular mechanisms have been widely documented. One of its prominent features is the role of dopaminergic systems in vertebrates and invertebrates. In mammals, dopamine has been extensively studied in the context of reward processing but is currently thought to be necessary and sufficient for the acquisition and expression of conditioned associations for both rewarding and aversive stimuli (Kutlu et al., 2022). *Drosophila* can learn to associate an odor (conditioned stimulus [CS]) with either sugar rewards or aversive electric shock (unconditioned stimulus [US]), in behaviors mediated by dopamine neurons (DANs) (Schwaerzel et al., 2003; Riemensperger et al., 2005; Claridge-Chang et al., 2009; Mao and Davis, 2009; Aso et al., 2010, 2012; Berry et al., 2012; Burke et al., 2012; C. Liu et al., 2012; Plaçais et al., 2012; Aso and Rubin, 2016; Adel and Griffith, 2021). Conditioned flies subsequently approach or avoid the reinforced odor. In the mushroom body, information about odors is sparsely encoded in subsets of Kenyon cells (KCs) (Honegger et al., 2011), which are divided into three subtypes that extend axons into the α/β, α'/β', and γ lobes (Crittenden et al., 1998). The domains of these lobes can be separated anatomically and

Received Nov. 20, 2022; revised Apr. 30, 2023; accepted May 27, 2023.

Author contributions: D.Y. and T.T. designed research; D.Y. and Y.M. performed research; D.Y. and Y.M. contributed unpublished reagents/analytic tools; D.Y. and T.T. analyzed data; D.Y. and T.T. wrote the first draft of the paper; D.Y. and T.T. edited the paper; T.T. wrote the paper.

This work was supported by Ministry of Education, Culture, Sports, Science and Technology Grant 21K06388 to D.Y. and Grant 19H03268 to T.T. and D.Y.; and the Takeda Science Foundation to T.T. We thank Yoshi Aso, Gerry Rubin, Serge Birman, and Taro Ueno for providing fly strains; Hitomi Takishita for maintaining fly stocks; and the Kyoto DGRC, the NIG Stock Center, the Bloomington Stock Center, and the Janelia Research Campus/HHMI for fly stocks.

The authors declare no competing financial interests.

Correspondence should be addressed to Daisuke Yamazaki at dyamazak@iqb.u-tokyo.ac.jp or Tetsuya Tabata at ttabata@iqb.u-tokyo.ac.jp.

https://doi.org/10.1523/JNEUROSCI.2152-22.2023

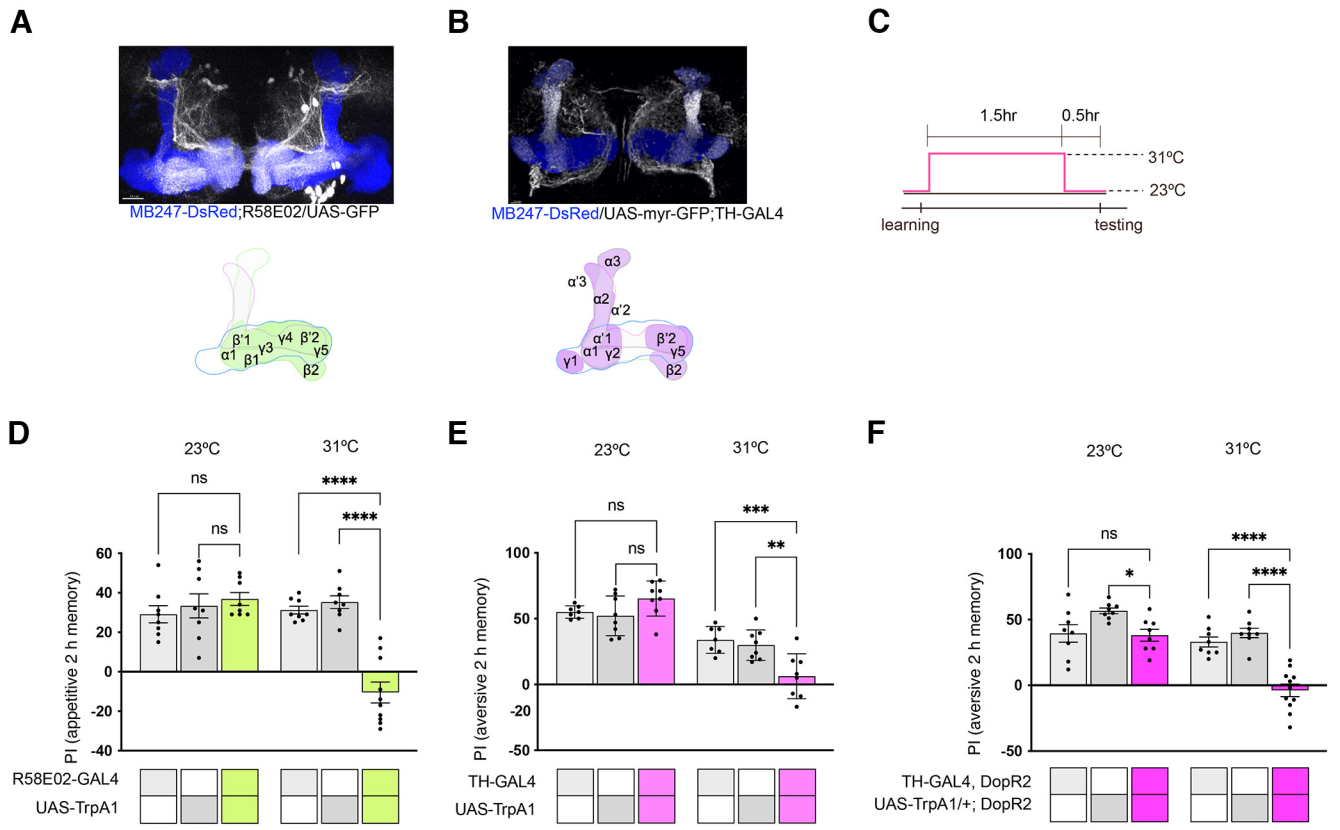

Figure 1. Outputs from DANs after conditioning decrease memory performance. ***A***, R58E02-GAL4-expressing UAS-GFP represents PAM DNAs shown in gray. Blue represents MB247-DsRed label KCs. Scale bar, 15 μm. Projections of DANs onto KCs are schematically indicated below. ***B***, TH-GAL4-expressing UAS-GFP represents both PPL1 and some PAM DNAs shown in gray. Projections of DANs onto KCs are schematically indicated below. Scale bar, 10 μm. The confocal images presented here and subsequently are compressed, and contrasts are nonlinearly adjusted for visibility. ***C***, Diagram represents a not-to-scale drawing of the temperature settings. ***D***, R58E02-GAL4-driven TrpA1 decreased the performance of appetitive 2 h memory when the temperature was raised to 31°C immediately after conditioning until 30 min before testing compared with the groups of genetic controls and permissive controls kept at 23°C. $\alpha = 0.05$, $n = 8$-10 for each. Temperature shift effects, $F_{(1,44)} = 16.17$, $p = 0.0002$; genotype effects, $F_{(2,44)} = 13.37$, $p < 0.0001$; interaction, $F_{(2,44)} = 21.71$. R58E02-GAL4 versus R58E02-GAL4/UAS-TrpA1, $q = 9.827$, $p < 0.0001$; UAS-TrpA1 versus R58E02-GAL4/UAS-TrpA1, $q = 10.77$, $p < 0.0001$. ***E***, TH-GAL4-driven TrpA1 decreased the performance of aversive 2 h memory when the temperature was raised to 31°C immediately after conditioning until 30 min before testing compared with the groups of genetic and permissive controls kept at 23°C. $\alpha = 0.05$, $n = 7$ or 8 for each. Temperature shift effects, $F_{(1,40)} = 81.17$, $p < 0.0001$; genotype effects, $F_{(2,40)} = 1.756$ $p = 0.1858$; interaction, $F_{(2,45)} = 11.03$, $p = 0.0002$. TH-GAL4 versus TH-GAL4/UAS-TrpA1, $q = 5.884$, $p = 0.0005$; UAS-TrpA1 versus TH-GAL4/UAS-TrpA1, $q = 5.212$, $p = 0.0019$. ***F***, In the *DopR2* mutant background, TH-GAL4-driven TrpA1 decreased the performance of aversive 2 h memory when the temperature was raised to 31°C immediately after conditioning until 30 min before testing compared with the groups of genetic and permissive controls kept at 23°C. $\alpha = 0.05$, $n = 8$-11 for each. Temperature shift effects, $F_{(1,45)} = 33.62$, $p < 0.0001$; genotype effects, $F_{(2,45)} = 24.19$, $p < 0.0001$; interaction, $F_{(2,45)} = 8.231$, $p < 0.0001$. TH-GAL4, *DopR2/DopR2* versus UAS-TrpA1/+; TH-GAL4, *DopR2/DopR2*, $q = 8.433$, $p < 0.0001$; UAS-TrpA1/+; *DopR2/DopR2* versus UAS-TrpA1/+; TH-GAL4, *DopR2/DopR2*, $q = 1$, $p < 0.0001$. Data are mean ± SEM. Dots represent individual data points. *$p < 0.05$; ****$p < 0.0001$; Tukey *post hoc* test following two-way ANOVA.

functionally into 15 different nonoverlapping compartments, each innervated by distinct DAN populations (Tanaka et al., 2008; Aso et al., 2014b). The output of DANs modulates the strength of synaptic connections between the KC axon terminals and the corresponding MB output neurons (MBONs) in each compartment (Aso et al., 2014a; Hige et al., 2015; Cognigni et al., 2018; Hige, 2018; Modi et al., 2020; Adel and Griffith, 2021). Forward association elevates the intracellular cAMP level and depresses the KC-MBON signaling, while backward association potentiates the KC-MBON signaling (Handler et al., 2019). We found that γKCs can be further subdivided into two populations based on the cAMP response element (CRE)-dependent expression: CRE-positive γ neurons (γCRE-p) are labeled by CRE-GAL4, whereas CRE-negative γ neurons (γCRE-n) are not. The output of γCRE-p is required for the formation of negative associations and inhibits the formation of positive associations, whereas the output of γCRE-n is required for positive associations and inhibits negative associations (Yamazaki et al., 2018). These circuit mechanisms probably depend at least in part on multiple layers of recurrent circuit functions, including reciprocal inhibition between MBONs, between positive and negative DANs, and excitatory or inhibitory communication from MBONs to DANs, as comprehensively reviewed by Adel and Griffith (2021), as well as on axo-axonic connections between KCs (Okray et al., 2023). Although dopamine signaling plays a key role in this circuit function, a recent study revealed that another neural transmitter, nitric oxide (NO), acts as a co-transmitter in a subset of dopaminergic neurons and antagonizes dopaminergic signaling, thereby modulating memory dynamics (Aso et al., 2019). Here, we show that GABA and glutamate act as neural transmitters in subsets of PPL1 and PAM DANs, respectively, and modulate memory dynamics.

Materials and Methods

Fly strains. Fly strains were maintained with the standard cornmeal food at 24 ± 2°C and 50 ± 10% humidity under a 12 h:12 h light/dark cycle. The TH-GAL4 fly transgene was provided by Serge Birman. *DopR2* (Akiba et al., 2020) was provided by Taro Ueno. UAS-DopR2

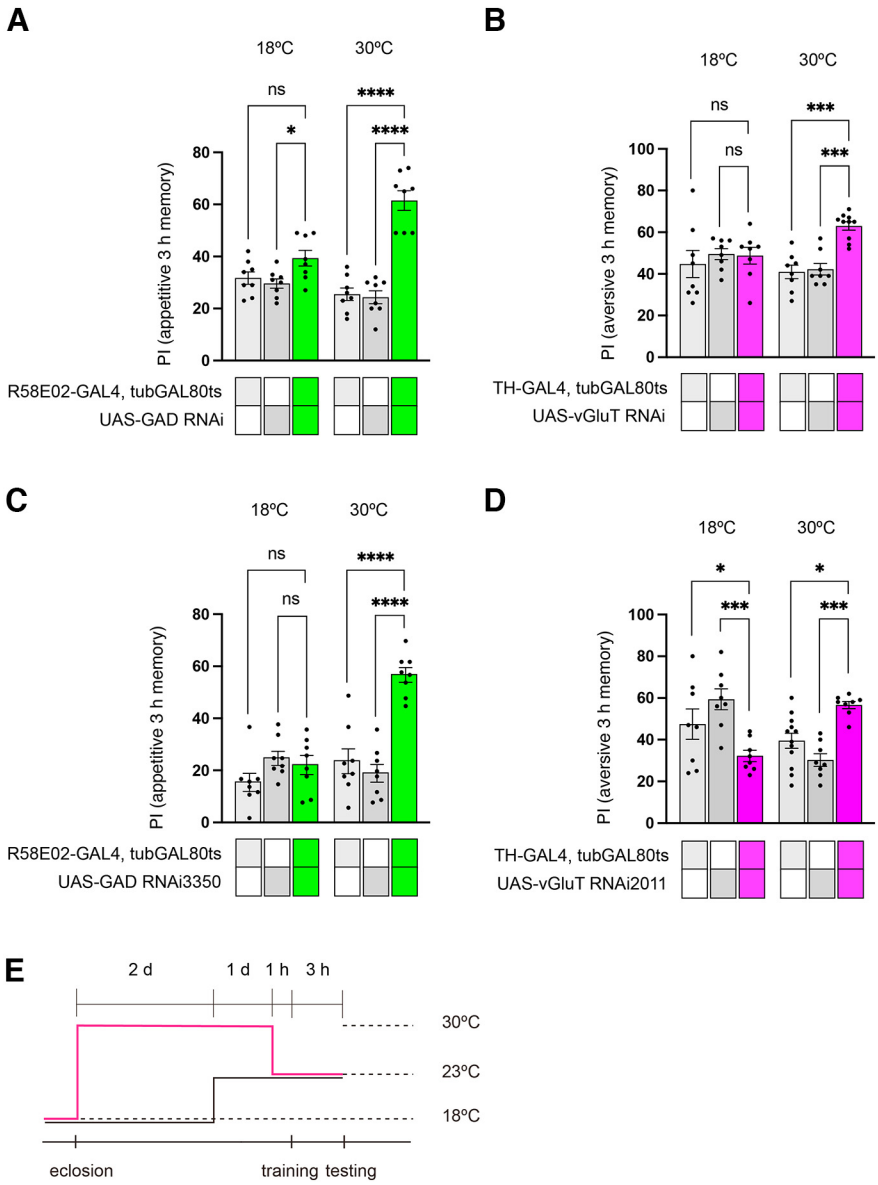

Figure 2. Knockdowns of vGluT in the PPL1 DANs and GAD in the PAM DANs potentiate aversive and appetitive memories, respectively. ***A***, R58E02-GAL4-driven UAS-GAD RNAi increased 3 h appetitive memory performance after tubGAL80ts was inactivated at 30°C for 3 d compared with the groups of genetic and permissive controls kept at 18°C. $\alpha = 0.05$, $n = 8$ for all. Temperature shift effects, $F_{(1,42)} = 2.542$, $p = 0.1184$; genotype effects, $F_{(2,42)} = 46.28$, $p < 0.0001$; interaction, $F_{(2,42)} = 17.51$, $p < 0.0001$. R58E02-GAL4, tubGAL80ts/+ versus UAS-GAD RNAi/+; R58E02-GAL4, tubGAL80ts/+, $q = 13.23$, $p < 0.0001$; UAS-GAD RNAi/+ versus UAS-GAD RNAi/+; R58E02-GAL4, tubGAL80ts/+, $q = 13.65$, $p < 0.0001$. ***B***, TH-GAL4-driven UAS-vGluT RNAi increased 3 h aversive memory performance after tubGAL80ts was inactivated at 30°C for 3 d, compared with the groups of genetic and permissive controls kept at 18°C. $\alpha = 0.05$, $n = 8$-10 for each. Temperature shift effects, $F_{(1,44)} = 0.1267$, $p = 0.7236$; genotype effects, $F_{(2,44)} = 6.983$, $p = 0.0023$; interaction, $F_{(2,44)} = 4.952$, $p = 0.0115$. TH-GAL4, tubGAL80ts/+ versus UAS-vGluT RNAi/+; TH-GAL4, tubGAL80ts/+, $q = 6.151$, $p = 0.0002$; UAS-vGluT RNAi/+ versus UAS-vGluT RNAi/+; TH-GAL4, tubGAL80ts/+, $q = 5.769$, $p = 0.0005$. ***C***, R58E02-GAL4-driven UAS-GAD RNAi3350 increased 3 h appetitive memory performance after tubGAL80ts was inactivated at 30°C for 3 d compared with the groups of genetic and permissive controls kept at 18°C. $\alpha = 0.05$, $n = 8$ for all. Temperature shift effects, $F_{(1,42)} = 18.30$, $p = 0.0001$; genotype effects, $F_{(2,42)} = 18.95$, $p < 0.0001$; interaction, $F_{(2,42)} = 16.87$, $p < 0.0001$. R58E02-GAL4, tubGAL80ts/+ versus UAS-GAD RNAi3350/+; R58E02-GAL4, tubGAL80ts/+, $q = 9.381$, $p < 0.0001$; UAS-GAD RNAi3350/+ versus UAS-GAD RNAi/+; R58E02-GAL4, tubGAL80ts/+, $q = 10.69$, $p < 0.0001$. ***D***, TH-GAL4-driven UAS-vGluT RNAi2011 increased 3 h aversive memory performance after tubGAL80ts was inactivated at 30°C for 3 d, compared with the groups of genetic and permissive controls kept at 18°C. $\alpha = 0.05$, $n = 8$-12 for each. Temperature shift effects, $F_{(1,46)} = 1.464$, $p = 0.2325$; genotype effects, $F_{(2,46)} = 0.06{,}182$, $p = 0.9401$; interaction, $F_{(2,46)} = 18.68$, $p < 0.0001$. TH-GAL4, tubGAL80ts/+ versus UAS-vGluT RNAi2011/+; TH-GAL4, tubGAL80ts/+ with heat shock, $q = 4.273$, $p = 0.0112$; UAS-vGluT RNAi2011/+ versus UAS-vGluT RNAi/+; TH-GAL4, tubGAL80ts/+ with heat shock, $q = 5.978$, $p = 0.0003$. Data are mean ± SEM. Dots represent individual data points. *$p < 0.05$; ***$p < 0.001$; ****$p < 0.0001$; Tukey *post hoc* test following two-way ANOVA. ***E***, Diagram represents a not-to-scale drawing of the temperature settings.

miR (Q. Liu et al., 2017) was provided by Mark Wu. hs-dCREB2b (Yin et al., 1994) was provided by Minoru Saitoe. UAS-vGluT RNAi (#104324), UAS-mGluR RNAi (#103736), UAS-GAD RNAi (#32344), and UAS-DopR2 RNAi (#105324) were obtained from the Vienna Drosophila RNAi Center. UAS-Rdl RNAi (#52903), UAS-vGluT RNAi 2011 (#40845), UAS-GAD RNAi 3350 (#51794), tubGAL80ts (#7018), R58E02-GAL4 (#41347), R58E02-LexA (#52740), MB320C (#68253), and MB296B (#68308) were procured from the Bloomington Drosophila Stock Center (Indiana University).

Construction of the TH-LexA driver. The fragments encoding the TH-5′, LexA-VP16, and TH-3′ regions were amplified from the genome of TH-GAL4 and MB247-LexA flies to generate TH-LexA-VP16. PCRs were performed with the following primers. Acquired fragments were integrated into the pBPGUw vector, in which the

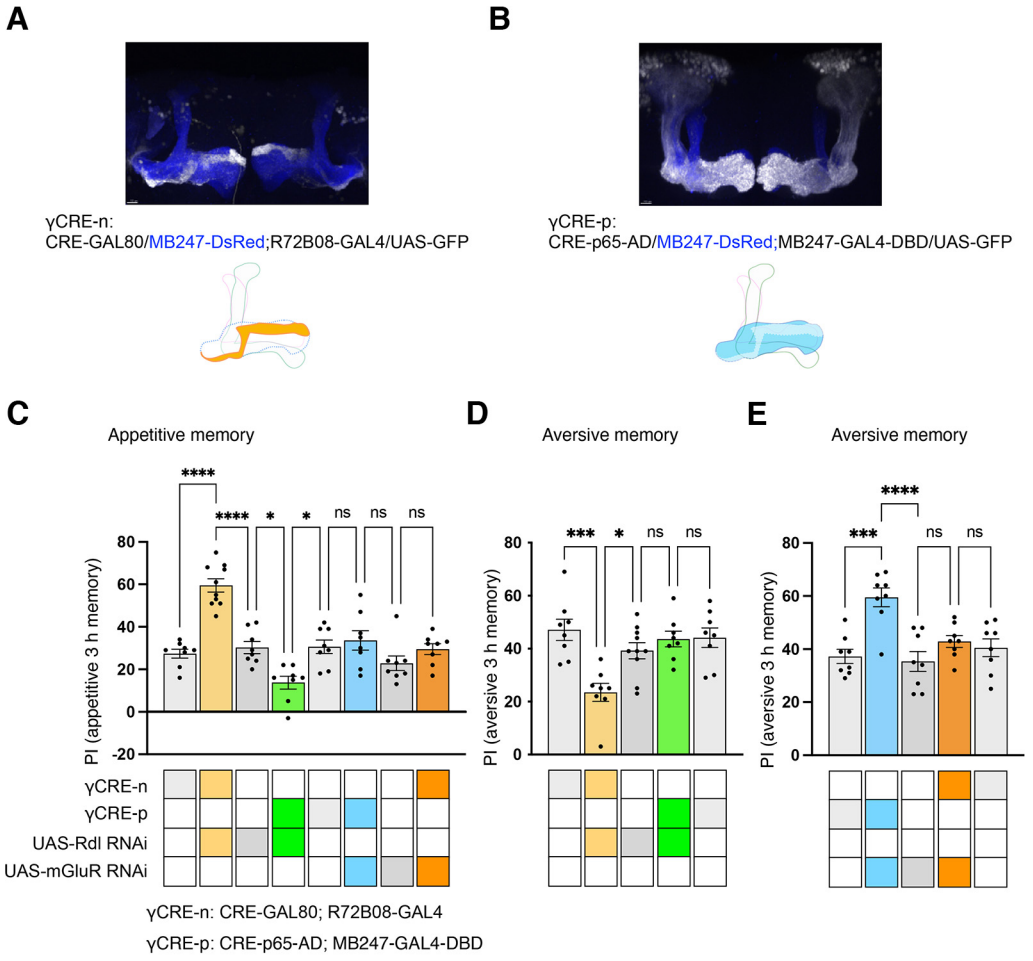

F

Memory	Appetitive memory				Aversive memory			
Cell type	γCRE-n		γCRE-p		γCRE-n		γCRE-p	
RNAi target	mGluR	Rdl	mGluR	Rdl	mGluR	Rdl	mGluR	Rdl
PI	-	↑	-	↓	-	↓	↑	-

Figure 3. In γCRE-n, Rdl knockdown potentiates appetitive memory, and mGluR knockdown in γCRE-p potentiates aversive memory. ***A***, CRE-GAL80; R72B08-GAL4 (hereinafter referred to as CRE-n) expressing UAS-GFP labels γCRE-n, shown in gray. Blue represents MB247-DsRed label KCs. Scale bar, 15 μm. γCRE-n is schematically indicated below. ***B***, CRE-p65-AD; MB247-GAL4-DBD (hereinafter referred to as CRE-p) expressing UAS-GFP represents γCRE-p in gray. Blue represents MB247-DsRed label KCs. Scale bar, 15 μm. γCRE-p is schematically indicated below. ***C***, CRE-n-driven UAS-Rdl RNAi increased appetitive 3 h memory, whereas CRE-p-driven UAS-Rdl RNAi decreased appetitive 3 h memory compared with genetic controls. $\alpha = 0.05$, $n = 8$-10 for each. $F_{(7,58)} = 19.13$, $p < 0.0001$. γCRE-n/+ versus γCRE-n/UAS-Rdl RNAi, $q = 10.48$, $p < 0.0001$; UAS-Rdl RNAi/+ versus γCRE-n/UAS-Rdl RNAi, $q = 9.546$, $p < 0.0001$. γCRE-p/+ versus γCRE-p/UAS-Rdl RNAi, $q = 5.225$, $p = 0.0108$; UAS-Rdl RNAi/+ versus γCRE-p/UAS-Rdl RNAi, $q = 5.109$, $p = 0.0138$. ***D***, CRE-n-driven UAS-Rdl RNAi decreased aversive 3 h memory, whereas CRE-p driving UAS-Rdl RNAi had no effect compared with genetic controls. $\alpha = 0.05$, $n = 8$ for all. $F_{(4,37)} = 7.271$, $p < 0.0002$. γCRE-n/+ versus γCRE-n/UAS-Rdl RNAi, $q = 6.784$, $p = 0.0002$; UAS-Rdl RNAi/+ versus γCRE-n/UAS-Rdl RNAi, $q = 4.753$, $p < 0.0147$. ***E***, CRE-p-driven UAS-mGluR RNAi increased aversive 3 h memory, whereas CRE-n driving UAS-Rdl mGluR had no effect compared with genetic controls. $\alpha = 0.05$, $n = 8$ for all. $F_{(4,35)} = 9.241$, $p < 0.0001$. γCRE-p/+ versus γCRE-p/UAS-mGluR RNAi, $q = 7.036$, $p = 0.0002$; UAS-mGluR RNAi/+ versus γCRE-p/UAS-mGluR RNAi, $q = 7.629$, $p < 0.0001$. Data are mean ± SEM. Dots represent individual data points. *$p < 0.05$; ***$p < 0.001$; ****$p < 0.0001$; Tukey *post hoc* test following one-way ANOVA. ***F***, Results are summarized in the panel.

transcription terminator was replaced by SV40, using the InFusion reagent (Clontech). TH-5′-forward: 5′-GAAAAGTGCCACCTGACG TCGCTGCAGTGACTCTGGGATT-3′; TH-5′-reverse: 5′-CGTTA ACGCTTTCATGGTACCGGATCCTTTCGCGAACTCGA-3′; LexA-forward: 5′-ATGAAAGCGTTAACGGCCAGGC-3′; LexA-reverse: 5′-TCCTCTAGAGGTACCCTACCCACCGTACTCGTCAATTC-3′; TH-3′-forward: 5′-TGTCTGGATCAAGCTTGAATTCGAGAGTCGAG AGTTCTTG-3′; and TH-3′-reverse: 5′-CGGTATCGATAAGCTT ATTCGATACATCTGTCCCTTATCG-3′.

Behavioral assays. Single-cycle olfactory conditioning assays were performed according to the standard methods (Tully and Quinn, 1985; Keene et al., 2006). For both aversive and appetitive conditioning, >50 flies were used for each experiment. In the case of aversive conditioning, flies were transferred to fresh food vials on the day before the training session. In the training session, flies were transferred to the conditioning chambers with electrodes wired on the inside and exposed to the first odor (CS^+) with 12 electric pulses (1.5 s duration of 60 V with 3.5 s interval), followed by the second odor as CS^-. Short-duration conditioning was performed according to the previously reported method (Beck et al., 2000). The 1× trial was 5 s odor exposure with 1.5 s electric shock, and a proportional number of shocks were presented at the same frequency followed by CS^- odor exposure of the same duration, after a 45 s fresh air interval. For appetitive conditioning, flies were transferred to the starvation vials with wet Kimwipes for 36-48 h before conditioning. In the appetitive training session, flies were exposed to the CS^- odor without sugar solution for 2 min. After a 45 s interval, the flies were transferred to the conditioning chamber containing filter paper soaked with 2 M sucrose with CS^+ odor exposure for 2 min. Behavioral data were

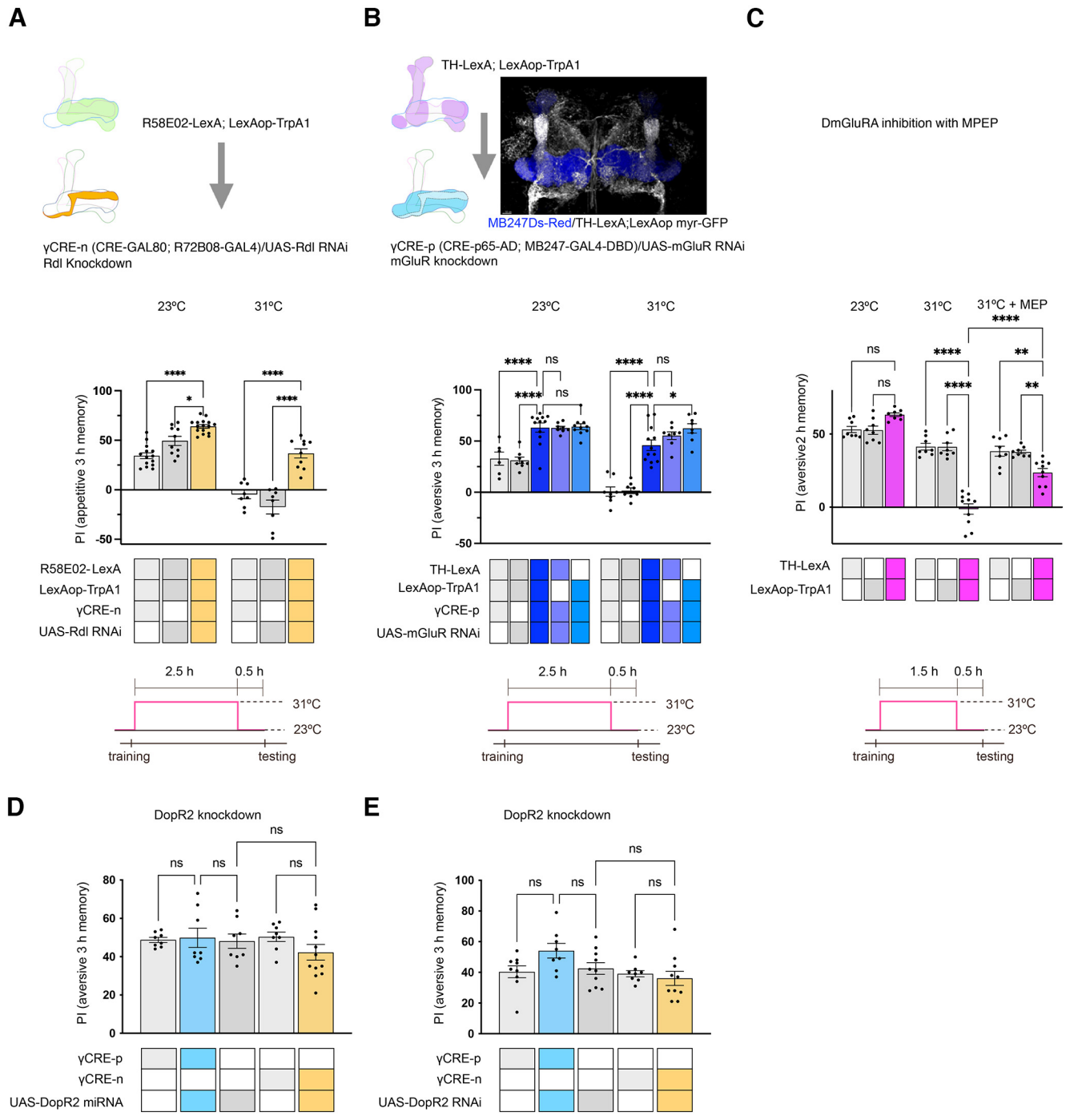

Figure 4. GABA inhibits appetitive memory through Rdl and glutamate inhibits aversive memory through mGluR. ***A***, Knockdown of Rdl in γCRE-n restored the appetitive 3 h memory impaired by R58E02-LexA-driven LexAop TrpA1. The flies harboring R58E02-LexA-driven LexAop TrpA1 and CRE-n-driven UAS-Rdl RNAi showed higher scores of appetitive 3 h memory at the permissive temperature compared with genetic controls (23°C). The same flies partially restored appetitive 3 h memory at restrictive temperatures, whereas the genetic controls showed no memory (31°C). $\alpha = 0.05$, $n = 8$-16 for each. Temperature shift effects, $F_{(1,60)} = 181.3$, $p < 0.0001$; genotype effects, $F_{(2,60)} = 55.03$, $p < 0.0001$; interaction, $F_{(2,60)} = 12.32$, $p < 0.0001$. UAS-Rdl RNAi/R58E02-LexA; LexAop-TrpA1/+ versus UAS-Rdl RNAi/R58E02-LexA; γCRE-n/LexAop-TrpA1, $q = 12.49$, $p < 0.0001$; R58E02-LexA/+; γCRE-n/LexAop-TrpA1 versus UAS-Rdl RNAi/R58E02-LexA; γCRE-n/LexAop-TrpA1, $q = 9.582$, $p < 0.0001$. ***B***, Knockdown of mGluR in γCRE-p restored the aversive 3 h memory impaired by TH-LexA driving LexAop TrpA1. TH-LexA-expressing LexAop myr-GFP represents both PPL1 and some PAM DNAs shown in gray. Scale bar, 10 μm. Top, The flies carrying CRE-p-driven UAS-mGluR RNAi exhibited elevated levels of aversive 3 h memory at the permissive temperature, relative to their genetic controls, regardless of the presence or absence of TH-LexAop-driven LexAop-TrpA (23°C). The same flies partially restored aversive 3 h memory, whereas the genetic controls showed no memory (31°C). $\alpha = 0.05$, $n = 6$-12 for each. Temperature shift effects, $F_{(1,78)} = 41.43$, $p < 0.0001$; genotype effects, $F_{(4,78)} = 55.56$, $p < 0.0001$; interaction, $F_{(4,78)} = 4.477$, $p = 0.0026$. TH-LexA/+; LexAop-TrpA1/γCRE-p versus TH-LexA/UAS-mGluR RNAi; LexAop-TrpA1/γCRE-p at 23°C, $q = 6.810$, $p < 0.0001$; UAS-mGluR RNAi/+; LexAop-TrpA1/γCRE-p at 23°C, $q = 7.881$, $p < 0.0001$; TH-LexA/+; LexAop-TrpA1/γCRE-p versus TH-LexA/UAS-mGluR RNAi; LexAop-TrpA1/γCRE-p at 31°C, $q = 11.14$, $p < 0.0001$; UAS-mGluR RNAi/+; LexAop-TrpA1/γCRE-p versus TH-LexA/UAS-mGluR RNAi; LexAop-TrpA1/γCRE-p at 31°C, $q = 10.92$, $p < 0.0001$. TH-LexA/UAS-mGluR RNAi; LexAop-TrpA1/γCRE-p versus UAS-mGluR/+; LexAop-TrpA1/γCRE-p at 31°C, $q = 0.2185$, $p = 0.0418$. ***C***, TH-LexA-driven LexAop-TrpA1 impaired aversive 2 h memory at 31°C, whereas the administration of MPEP partially restored the memory (31°C + MPEP). $\alpha = 0.05$ $n = 8$-10 for each. Temperature shift or drug effects, $F_{(2,67)} = 96.45$, $p < 0.0001$; genotype effects, $F_{(2,67)} = 35.02$, $p < 0.0001$; interaction, $F_{(4,67)} = 33.30$, $p < 0.0001$. TH-LexA/+ versus TH-LexA/LexAop-TrpA1 at 31°C, $q = 16.34$, $p < 0.0001$; LexAop-TrpA1/+ versus TH-LexA/LexAop-TrpA1 at 31°C, $q = 16.29$, $p < 0.0001$; TH-LexA/+ versus TH-LexA/LexAop-TrpA1 with MPEP at 31°C, $q = 5.610$, $p = 0.0053$; LexA-TrpA1/+ versus TH-LexA/LexAop-TrpA1 with MPEP at 31°C,

acquired by independent trials, using flies collected from independent crossings.

Temperature shift experiments. In the case of activation of DANs with dTrpA1 during the memory consolidation step, trained flies were transferred to the incubator without preheating until 30 min before the test session at 31°C. For the gene inductions using tubGAL80^{ts}, flies were crossed at 18°C until adult eclosion, collected, and raised at 30°C for 3 d until the behavioral assays. For dCREB2b induction by heat shock, flies were raised at 37°C for 30 min. After 3 h interval at 23°C, single-cycle training was performed following previous reports (Perazzona et al., 2004). For cold shock assays, 2 h after a single cycle of aversive conditioning, flies were transferred to vials cooled on ice and kept there for 2 min. They were then placed in their "home" vials at 23°C for another 1 h until the test session at 23°C.

Reagent feeding. Cycloheximide (WAKO) was dissolved in 100 mM sucrose to achieve a 35 mM CHX solution. Flies were transferred to vials containing a Kimwipe soaked in 300 μl of CHX solution for 16-20 h until aversive conditioning. 2-Methyl-6-(phenylethynyl) pyridine (MPEP; 100 μM) and pCPA (10 mg/ml) were fed in the same manner, following the previous reports (McBride et al., 2005; Lee et al., 2011; Plaçais et al., 2012).

Histology. Driver lines were visualized using MB247-DsRed;R58E02/UAS-GFP (PAM DANs), MB247-DsRed/UAS-myr-GFP;TH-GAL4 (PPL1 DANs), CRE-GAL80/MB247-DsRed;R72B08/UAS-GFP (γCRE-n), CRE-p65-AD/MB247-DsRed; MB247-GAL4-DBD/UAS-GFP (γCRE-p), MB247-DsRed/TH-LexA;LexAop myr-GFP (PPL1 DANs), MB247-DsRed;MB320C/UAS-GFP (γ1ped DAN), and MB296B/MB247-DsRed; UAS-GFP (γ2α1 DAN). The images of brains fixed in 4% formaldehyde were acquired using a Zeiss LSM710 confocal microscope and processed by the Imaris software. Stacks of 3D images were visualized with the maximum projection intensity method. A nonlinear contrast stretch was applied to adjust intensities.

Statistics. Statistical analyses were performed by using GraphPad Prism 9. Behavioral data are shown as mean ± SEM. Multiple comparisons were performed by Tukey's *post hoc* test after ANOVA.

Results

DANs inhibit olfactory memories when exogenously activated after conditioning

PAM DANs project to the horizontal lobes (Burke et al., 2012; C. Liu et al., 2012; Yamagata et al., 2015) of KCs and signal the presence of appetitive stimuli during the acquisition of olfactory memory in *Drosophila*, whereas PPL1 DANs project to the vertical lobes of KCs and signal the presence of aversive stimuli (Waddell, 2005; Mao and Davis, 2009; Aso et al., 2010, 2012; Berry et al., 2012; Aso and Rubin, 2016). We previously showed that the γKCs could be subdivided into γCRE-p and γCRE-n, and the output from γCRE-p is indispensable for aversive memory consolidation, while that from γCRE-n is required for appetitive memory consolidation (Yamazaki et al., 2018). During our studies to determine whether DANs are involved in these processes, we confirmed that the PAM (Fig. 1*A*) and PPL1 DANs (Fig. 1*B*) exogenously activated with the transient receptor potential cation channel A1, dTrpA1 (Hamada et al., 2008), after conditioning, impeded aversive and appetitive memories, respectively (Fig. 1*C*,*D*), when expressed after conditioning by using the GAL4/UAS system (Brand and Perrimon, 1993), as reported (Berry et al., 2012; Plaçais et al., 2012). We then tested whether the dopamine receptor DopR2 (DAMB) mediates this inhibitory role, since it is involved in active forgetting (Berry et al., 2012). The activation of PPL1 DANs in the null *DopR2* mutant (Akiba et al., 2020) background still impaired aversive memory (Fig. 1*F*), suggesting that another transmitter plays an inhibitory role in DANs.

GABA and glutamate as co-transmitters of DANs negatively regulate memory

The recent findings by Aso et al. (2019) that NO acts as a co-neurotransmitter in a subset of PPL1 DANs, as well as studies on vertebrate dopaminergic neurons that can co-transmit glutamate and GABA (Granger et al., 2017), prompted us to search for co-transmitters in DANs. Based on the transcriptomic analysis (Aso et al., 2019) and the chemoconnectomics (Deng et al., 2019), we reasoned that PAM DANs could co-transmit GABA. The glutamate transporter (vGluT) has been identified in a subset of PPL1 DANs (Aguilar et al., 2017; Aso et al., 2019). To examine the possible functions of the co-transmitters, we decreased the expression of glutamate decarboxylase (GAD), which catalyzes glutamate conversion to GABA, and vGluT by RNA interference (RNAi) (Ameres and Zamore, 2013) in PAM and PPL1 DANs, respectively, before conditioning using the TARGET system (McGuire et al., 2003) to restrict the expression of the RNAi construct to the adult stage, to prevent developmental effects. The knockdown of GAD in the PAM DANs, using the R58E02-GAL4 driver (Jenett et al., 2012), facilitated appetitive 3 h memory (Fig. 2*A*), whereas the knockdown of vGluT in the PPL1 DANs using the TH-GAL4 driver (Friggi-Grelin et al., 2003) facilitated aversive 3 h memory (Fig. 2*B*), suggesting that these transmitters negatively regulate appetitive and aversive memories, respectively. It should be noted that TH-GAL4 labels not only PPL1 DANs but also some PAM DANs that project to α1, β2, β'2, and γ5 (Aso et al., 2012). These results were confirmed by using independent RNAi lines for GAD (Fig. 2*C*) and vGluT (Fig. 2*D*).

The GABA receptor rdl and the mGluR DmGluRA in γKCs are responsible for the negative regulation of memory

To further examine the roles of the co-transmitters, we next searched for their receptors and target cells. To this end, we analyzed the roles of the Rdl (Resistance to dieldrin) GABA-A receptor (Ffrench-Constant et al., 1992; X. Liu et al., 2007) and the DmGluRA glutamate receptor (Parmentier et al., 1996). We reasoned that the γKCs are the first candidates for the targets of these co-transmitters, since memory defects caused by the dopamine receptor mutation, *dumb2*, are rescued by the expression of the WT dopamine receptor in γKCs (Qin et al., 2012). As described, γKCs can be subdivided into γCRE-n and γCRE-p (Yamazaki et al., 2018). γCRE-n is defined by the combination of CRE-GAL80 (GAL80 transcriptional inhibitor controlled by the CRE sequence) and R72B08 GAL4 (γKC-specific GAL4) (Fig. 3*A*). γCRE-p is defined by the split GAL4 system (Luan et al., 2006) consisting of CRE-p65-AD (p65 transcriptional activation domain under the control of the CRE sequence) and MB247-GAL4-DBD (GAL4 DNA-binding domain under the control of the MB-specific sequence 247; Fig. 3*B*) (Zars et al., 2000). We expressed RNAi constructs targeting DmGluRA or Rdl in either γCRE-n or γCRE-p and searched for the combinations that facilitate memory formation. The knockdown of Rdl in

←

$q = 5.419$, $p = 0.0082$; comparison of TH-LexA/LexAop-TrpA1 with or without MPEP at 31°C, $q = 10.11$, $p < 0.0001$. ***D***, Knockdown of DopR2 in γKCs did not affect 3 h aversive memory. Short hairpin RNAi (Q. Liu et al., 2017) was expressed in γCRE-p or γCRE-n KCs. $\alpha = 0.05$, $n = 8$-12 for each. $F_{(4,39)} = 0.9166$, $p = 0.4640$. ***E***, Knockdown of DopR2 by an RNAi construct (105324) in γKCs did not affect 3 h aversive memory. $\alpha = 0.05$, $n = 8$-10 for each. $F_{(4,40)} = 2.784$, $p = 0.0394$. Data are mean ± SEM. Dots represent individual data points. *$p < 0.05$; **$p < 0.01$; ****$p < 0.0001$; Tukey *post hoc* test following two-way ANOVA. Diagram represents a not-to-scale drawing of the temperature settings (***A–C***, bottom).

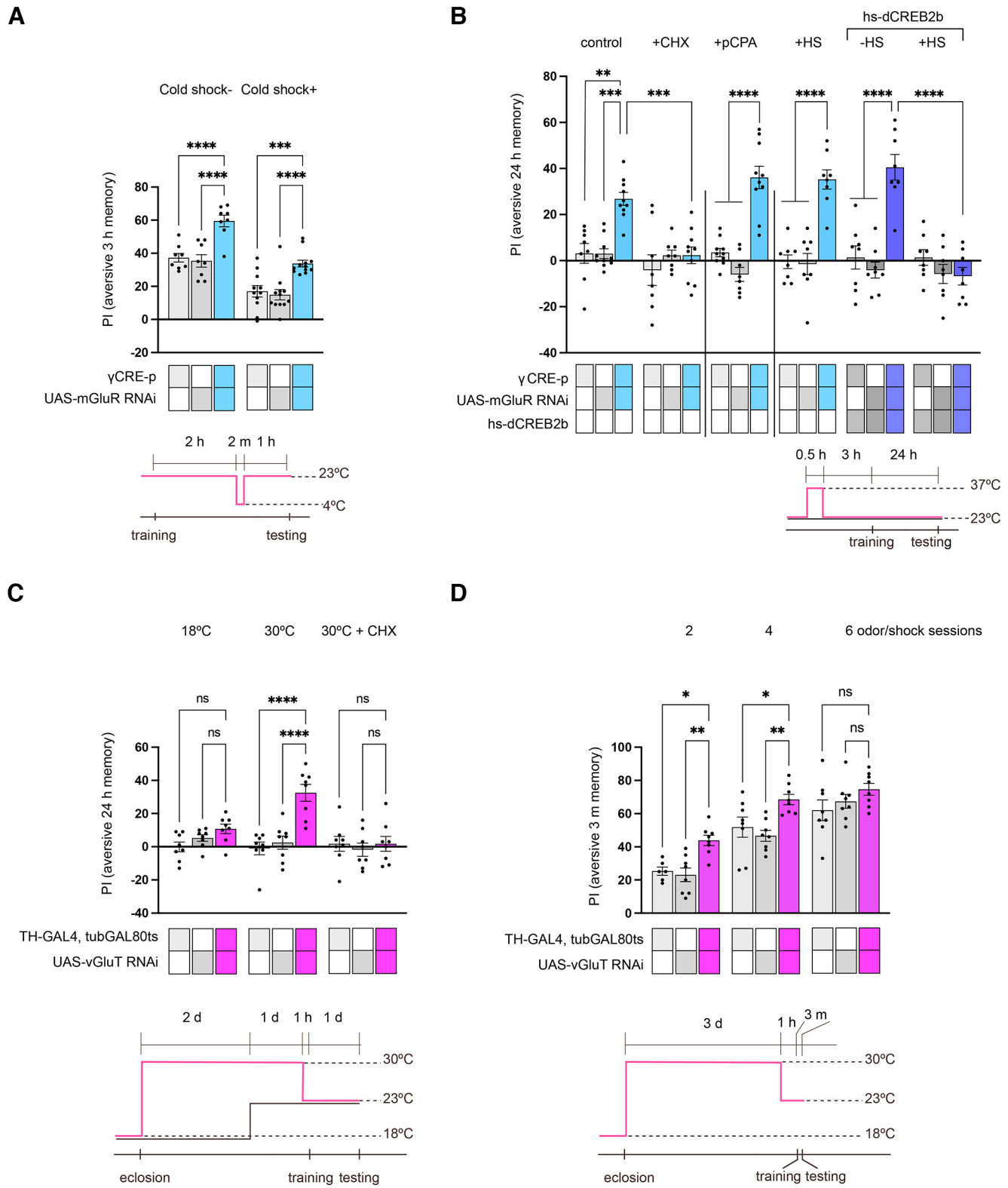

Figure 5. Attenuating the glutamate signaling from PPL1 DANs facilitates the formation of anesthesia-resistant memory, long-term memory, and learning. ***A***, Knockdown of mGluR in γCRE-p potentiated aversive 3 h memory compared with genetic controls, with and without cold shock. $\alpha = 0.05$, $n = 8$-12 for each. Cold shock effects, $F_{(1,53)} = 73.50$, $p < 0.0001$; genotype effects, $F_{(2,53)} = 28.36$, $p < 0.0001$; interaction, $F_{(2,53)} = 0.4877$, $p = 0.6168$. γCRE-p/+ versus γCRE-p/UAS-mGluR RNAi without cold shock, $q = 6.457$, $p < 0.0001$; UAS-mGluR RNAi/+ versus γCRE-p/UAS-mGluR RNAi without cold shock, $q = 7.001$, $p < 0.0001$; γCRE-p/+ versus γCRE-p/UAS-mGluR RNAi with cold shock, $q = 5.823$, $p = 0.0004$; UAS-mGluR RNAi/+ versus γCRE-p/UAS-mGluR RNAi with cold shock, $q = 6.694$, $p < 0.0001$. ***B***, Knockdown of mGluR in γCRE-p forms 24 h aversive memory after a single cycle of training (control), which was sensitive to the administration of cycloheximide (+CHX), while insensitive to pCPA (serotonin blocker) administration (+pCPA). Dominant-negative CREB (dCREB2b) expression abolished 24 h aversive memory formed by mGluR knockdown (+HS). The administration of CHX or pCPA experiments, as well as heat shock (HS) experiments, were conducted independently. The results of CHX, pCPA, and the control HS were collectively subjected to ANOVA, while the hs-dCREB2b results underwent separate ANOVA and were visually represented in a graph. $\alpha = 0.05$, $n = 8$-10 for each. CHX, pCPA or HS effects, $F_{(3,\ 94)} = 6.230$, p = 0.0007; genotype effects, $F_{(2,\ 94)} = 61.39$, $p < 0.0001$; interaction, $F_{(6,\ 94)} = 6.757$, $p < 0.0001$. γCRE-p/+ versus γCRE-p/ UAS-mGluR RNAi in the control, $q = 6.326$, $p = 0.0012$; UAS-mGluR RNAi/+ versus γCRE-p/ UAS-mGluR RNAi

γCRE-n facilitated appetitive memory and that of DmGluRA in γCRE-p facilitated aversive memory, whereas the knockdowns of Rdl in γCRE-p and γCRE-n decreased appetitive and aversive memories, respectively (Fig. 3*C–F*). These results suggested that glutamate released from PPL1 attenuates aversive memory through DmGluRA, and GABA released from PAM attenuates appetitive memory through Rdl, since γCRE-n mainly functions in appetitive memory and γCRE-p is involved in aversive memory (Yamazaki et al., 2018). This was confirmed in the following experiments. Although the appetitive and aversive memories were compromised when the PAM and PPL1 DANs were thermo-genetically activated, respectively (Fig. 1), these inhibitory effects were partially alleviated when Rdl was knocked down in γCRE-n and DmGluRA was knocked down in γCRE-p, respectively (Fig. 4*A*,*B*). These results support the proposals that (1) glutamate is a co-transmitter of PPL1 DANs and negatively modulates the aversive memory through mGluR in γCRE-p; and (2) GABA is a co-transmitter of PAM DANs and negatively modulates the appetitive memory through Rdl in γCRE-n. We further tested the inhibitory role of DmGluRA, using the antagonist MPEP (Kanellopoulos et al., 2012). The administration of MPEP partially restored the aversive memory when PPL1 DANs were thermo-genetically activated after conditioning (Fig. 4*C*), confirming the role of DmGluRA.

It should be noted that vGluT facilitates DA loading into the synaptic vesicle, where vGluT and vesicular monoamine transporter (vMAT) are colocalized, and this is also the case for PPL1 neurons. Aguilar et al. (2017) reported that vGluT and vMAT are colocalized in part of the terminals of MB-MV1 ($\gamma 2\alpha' 1$) neurons in the PPL1 cluster. The results obtained with the vGluT knockdown could thus formally be ascribed, at least in part, to the decrease in the DA release. However, the inhibitory effect was alleviated when DmGluRA (Fig. 4*B*) but not DopR2 (Fig. 1*F*), was knocked down in γCRE-p, indicating that the inhibitory role of the PPL1 neurons described here is mediated by the glutamate signaling. It should also be noted that the NMDA receptor expressed in KCs probably does not play a role in this pathway, since the knockdown of the essential subunit of the NMDA receptor, dNR1, compromises learning (Xia et al., 2005), and thus this phenotype is contrary to what we observed by knocking down vGluT.

Consequently, we revisited the role of DopR2 in the context of aversive memory specifically in γKCs, considering that the knockdown of DmGluRA is sufficient to increase the memory score. For this purpose, we conducted RNA interference experiments using validated RNAi lines. Knocking down DopR2 via a DopR2 miRNA or an RNAi in γ CRE-p KCs did not exert a significant impact on the aversive memory score (Fig. 4*D*,*E*). We decided to focus our efforts on the glutamate-DmGluRA system in aversive memory since X. Liu et al. (2007, 2009) already revealed the inhibitory role of Rdl in KCs. Our data suggested that PAM DANs are the likely candidates for the source of GABA.

A single cycle of conditioning is sufficient to induce long-term memory when the DmGluRA signal is impaired

Aversive olfactory memories can be classified according to their stabilities. After a single cycle of conditioning, two phases of mid-term memory can be defined by their resistance to cold shock treatment (Qin et al., 2012), and are referred to as anesthesia-sensitive memory and anesthesia-resistant memory. We examined the nature of the aversive memory facilitated by knocking down the mGluR system. The flies with DmGluRA knocked down in γCRE-p were kept for 2 min on ice, 2 h after a single cycle of aversive conditioning, and examined for memory performance 3 h after conditioning. The anesthesia-resistant memory component was increased compared with the genetic controls (Fig. 5*A*). We then asked whether the knockdown of the glutamatergic system elicits more stable long-term memory after a single cycle of conditioning. In the WT, multiple cycles of aversive conditioning with intervals result in the formation of long-term memory lasting longer than 24 h and require new protein synthesis for its formation (Tully et al., 1994). The 24 h memory was indeed observed even after a single cycle of conditioning when DmGluRA in γCRE-p (Fig. 5*B*) or vGluT in the PPL1 DANs (Fig. 5*C*) was knocked down, and was completely blocked after feeding the flies with cycloheximide (+CHX), a *de novo* protein synthesis inhibitor. To rule out the potential contribution of anesthesia-resistant memory enhancement, we additionally investigated the impact of p-chlorophenylalanine, a serotonin blocker that destabilizes anesthesia-resistant memory, and observed no such effect (+pCPA in Fig. 5*B*). Furthermore, the expression of the dominant negative form of CREB, dCREB2b, under the control of the heat-shock promoter (Yin et al., 1994) in the DmGluRA knocked down flies resulted in the complete inhibition of 24 h memory (+HS in Fig. 5*B*), indicating that the Glu/mGluR signaling knockdown-induced 24 h memory is contingent on the CREB activity.

Together, these findings suggest that the DmGluR pathway destabilizes consolidated aversive memory. We further investigated whether this pathway plays a role in learning per se, given that a deficit in learning rate has been observed in a *dfmr1* mutant that overexpresses DmGluR in KCs (for details, see Discussion). To assess the learning rate, we used a previously reported short-duration protocol (Beck et al., 2000) involving fewer US/CS pairings post-training than the standard protocol,

←

in the control, $q = 6.745$, $p = 0.0004$; γCRE-p/UAS-mGluR RNAi in the control versus γCRE-p/UAS-mGluR RNAi with CHX, $q = 6.943$, $p = 0.0002$; γCRE-p/+ versus γCRE-p/UAS-mGluR RNAi with pCPA, $q = 9.239$, $p < 0.0001$; UAS-mGluR RNAi/+ versus γCRE-p/UAS-mGluR RNAi with pCPA, $q = 11.25$, $p < 0.0001$; γCRE-p/+ versus γCRE-p/UAS-mGluR RNAi with HS, $q = 9.062$, $p < 0.0001$; UAS-mGluR RNAi/+ versus γCRE-p/UAS-mGluR RNAi with HS, $q = 9.315$, $p < 0.0001$. hs-dCREB2b effects, $F_{(1,42)} = 21.38$, $p < 0.0001$, genotype effects, $F_{(2,\ 42)} = 13.53$, $p < 0.0001$, interaction, $F_{(2,\ 42)} = 19.32$, $p < 0.0001$. hs-dCREB2b/+; γCRE-p/+ versus UAS-mGluR RNAi/hs-dCREB2b; γCRE-p/+ without HS, $q = 9.066$, $p < 0.0001$; UAS-mGluR RNAi/hs-dCREB2b versus UAS-mGluR RNAi/hs-dCREB2b; γCRE-p/+ without HS, $q = 10.34$, $p < 0.0001$; UAS-mGluR RNAi/hs-dCREB2b; γCRE-p/+ without HS versus UAS-mGluR RNAi/hs-dCREB2b; γCRE-p/+ with HS, $q = 10.95$, $p < 0.0001$. ***C***, Flies with TH-GAL4-driven UAS-vGluT RNAi in the presence of tubGAL80ts, raised at 30°C for 3 d just before training to inactivate tubGAL80ts, form aversive 24 h memory after a single-cycle of training (30°C), which is sensitive to the administration of cycloheximide (30°C +CHX). The same flies kept at 18°C did not form aversive 24 h memory after the same training (18°C). $\alpha = 0.05$, $n = 8$ for all. Heat shock effects, $F_{(2,63)} = 5.947$, $p = 0.0043$; genotype effects, $F_{(2,63)} = 13.53$, $p < 0.0001$; interaction, $F_{(4,63)} = 6.050$, $p = 0.0003$. TH-GAL4, tubGAL80ts/+ versus UAS-vGluT RNAi/+; TH-GAL4, tubGAL80ts/+ at 30°C, $q = 8.753$, $p < 0.0001$; UAS-vGluT RNAi/+ versus UAS-vGluT RNAi/+; TH-GAL4, tubGAL80ts/+ at 30°C, $q = 7.839$, $p < 0.0001$. ***D***, Short-duration training showed elevated learning efficacy by knocking down vGluT in PPL1 neurons. All fly lines were raised at 30°C for 3 d before conditioning. $\alpha = 0.05$. $n = 6$-8 for each. Training number effects, $F_{(2,61)} = 56.90$, $p < 0.0001$; genotype effects, $F_{(2,61)} = 14.69$, $p < 0.0001$; interaction, $F_{(4,61)} = 0.9861$, $p = 0.4219$. UAS-vGluT RNAi/+ versus UAS-vGluT RNAi/+; TH-GAL4, tubGAL80ts/+ in two sessions, $q = 4.920$, $p = 0.0027$; TH-GAL4/+; versus UAS-vGluT RNAi/+; TH-GAL4, tubGAL80ts/+ in two sessions, $q = 4.070$, $p = 0.0150$. UAS-vGluT RNAi/+ versus UAS-vGluT RNAi/+; TH-GAL4, tubGAL80ts/+ in four sessions, $q = 5.187$, $p = 0.0015$; TH-GAL4/+; versus UAS-vGluT RNAi/+; TH-GAL4, tubGAL80ts/+ in four sessions, $q = 3.942$, $p = 0.0191$. Data are mean ± SEM. Dots represent individual data points. *$p < 0.05$; **$p < 0.01$; ***$p < 0.005$; ****$p < 0.0001$; Tukey *post hoc* test following two-way ANOVA. Diagram represents a not-to-scale drawing of the temperature settings (bottom).

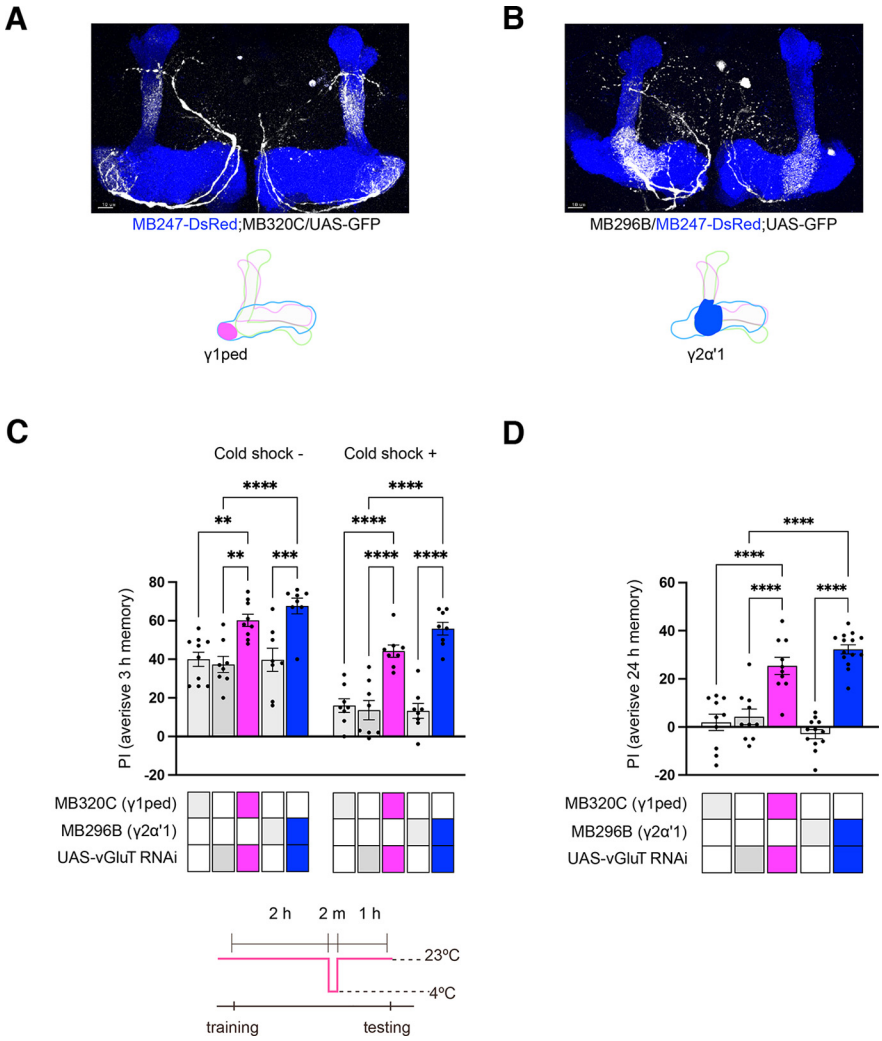

Figure 6. A single cycle of training can form anesthesia-resistant memory and long-term memory when vGluT is knocked down in either γ1pedc or $\gamma2\alpha'1$ DANs. ***A***, ***B***, MB320C and MB296B split GAL4-expressing UAS-GFP label γ1pedc (***A***) and $\gamma2\alpha'1$ DANs (***B***), respectively, shown in gray. Blue represents MB247-DsRed labeled KCs. Projections of DANs onto KCs are schematically indicated below. Scale bar, 10 μm. ***C***, vGluT RNAi driven by MB320C or MB296B split GAL4 generates stable 3 h memory partially resistant to cold shock after a single cycle training. $\alpha = 0.05$, $n = 8$-10 for each. Cold shock effects, $F_{(1,73)} = 61.95$, $p < 0.0001$; genotype effects, $F_{(4,73)} = 33.93$, $p < 0.0001$; interaction, $F_{(4,73)} = 1.143$, $p = 0.3432$. UAS-vGluT RNAi/+ versus MB320C/UAS-vGluT RNAi without cold shock, $q = 5.649$, $p = 0.0014$; MB320C/+ versus MB320C/UAS-vGluT RNAi without cold shock, $q = 5.287$, $p = 0.0033$; UAS-vGluT RNAi/+ versus MB296B/UAS-vGluT RNAi without cold shock, $q = 7.268$, $p < 0.0001$; MB296B/+ versus MB296B/UAS-vGluT RNAi without cold shock, $q = 6.697$, $p = 0.0001$; UAS-vGluT RNAi/+ versus MB320C/UAS-vGluT RNAi with cold shock, $q = 7.358$, $p < 0.0001$; MB320C/+ versus MB320C/UAS-vGluT RNAi with cold shock, $q = 6.787$, $p < 0.0001$; UAS-vGluT RNAi/+ versus MB296B/UAS-vGluT RNAi with cold shock, $q = 10.15$, $p < 0.0001$; MB296B/+ versus MB296B/UAS-vGluT RNAi with cold shock, $q = 10.24$, $p = 0.0001$. Diagram represents a not-to-scale drawing of the temperature settings (bottom). ***D***, MB320C or MB296B split GAL4 driving UAS-vGluT RNAi form 24 h aversive memory after a single cycle of training. $\alpha = 0.05$, $n = 10$-14 for each. $F_{(4,51)} = 35.31$, $p < 0.0001$. UAS-vGluT RNAi/+ versus MB320C/UAS-vGluT RNAi, $q = 7.327$, $p < 0.0001$; MB320C/+ versus MB320C/UAS-vGluT RNAi, $q = 8.122$, $p < 0.0001$; UAS-vGluT RNAi/+ versus MB296B/UAS-vGluT RNAi, $q = 10.48$, $p < 0.0001$; MB296B/+ versus MB296B/UAS-vGluT RNAi, $q = 13.86$, $p < 0.0001$. Data are mean ± SEM. Dots represent individual data points. $^{**}p < 0.01$; $^{***}p < 0.001$; $^{****}p < 0.0001$; Tukey *post hoc* test following ANOVA.

to improve the resolution for detecting variations in the learning rate. Our results revealed that the aversive memory score of flies with reduced DmGluR was significantly greater following 2 or 4 US/CS pairings compared with the genetic controls, but the difference was insignificant after 6 US/CS pairings, probably because of the ceiling effects under these experimental conditions (Fig. 5*D*). These results suggest that the DmGluR pathway decreases the learning rate.

PPL1 DANs consist of several neuron types, and γKC-projecting γ1pedc (also known as MB-MP1, Fig. 6*A*) and $\gamma2\alpha'1$ (also known as MB-MV1, Fig. 6*B*) are required for short- to mid-term memory formation (Aso et al., 2012). To discern which DANs are accountable for destabilizing memory via Glu/mGluR signaling, we measured the 3 h memory by knocking down vGluT in each neuron type, with or without cold shock. Our findings suggested that the vGluT knockdown in both cases led to improved memory consolidation that was resistant to cold shock 2 h after training, as illustrated in Figure 6*C*. We also examined the long-term memory performance of flies with vGluT knocked down in each of these neuron types, and found that a single cycle of conditioning was sufficient to form long-term memory in both cases (Fig. 6*D*), suggesting that inhibiting glutamate release from a single dopamine neuron type is sufficient to induce long-term memory formation after a single cycle of conditioning.

Discussion

The pivotal roles of dopaminergic neurons in the formation of *Drosophila* olfactory memory have been extensively studied and documented (Kim et al., 2007; Aso et al., 2010, 2012; Berry et al.,

2012; C. Liu et al., 2012; Aso and Rubin, 2016; Villar et al., 2022) and reviewed (Cognigni et al., 2018; Modi et al., 2020; Adel and Griffith, 2021). Two types of D1-like dopamine receptors, DopR1 (also known as Dop1R1 or Dumb) and DopR2 (also known as Dop1R2 or Damb), expressed in KCs play opposing roles in KC-MBON signaling, with DopR1 required for depression and DopR2 for potentiation (Handler et al., 2019). The DopR1 signaling plays a major role in forward training, and DopR2 serves in backward training and forgetting (Berry et al., 2012; Handler et al., 2019). Recent findings on co-transmitters, such as NO in PPL1-γ1pedc dopaminergic neurons, have illuminated yet another way of modulating memory formation (Aso et al., 2019). Accordingly, we hereby add glutamate and GABA to the list of their co-transmitters.

The mGluR signaling negatively modulates aversive memory

The role of DmGluRA in olfactory memory formation was revealed in studies of the gene *dfmr1*, which encodes an ortholog of RNA-binding fragile X protein (fragile X mental retardation protein) (Richter and Zhao, 2021). Fragile X mental retardation protein represses unregulated synaptic translation, and its loss results in a spectrum of cognitive deficits known as fragile X syndrome. *dfmr1* mutants reportedly result in excess DmGluRA activity (McBride et al., 2005), as found in mice (Huber et al., 2002) and cause learning and memory deficits (Bolduc et al., 2008). Kanellopoulos et al. (2012) demonstrated that *dfmr1* mutants increase the amount of DmGluRA and cause memory deficits, which were restored by knocking down DmGluRA in $\alpha\beta$ KCs. They also reported that cAMP levels in KCs were lower in *dfmr1* heterozygotes compared with the WT, and were restored to the WT level when DmGluRA was knocked down. DopR1 coupled with Gαs elevates the cAMP level, whereas DmGluRA is thought to be coupled with Gi/o and lowers the cAMP level (Kanellopoulos et al., 2012). This is at least partly in line with our findings that DmGluRA plays an antagonistic role with the DopR1-mediated dopamine signaling, except that Kanellopoulos et al. (2012) showed the inhibiting role of DmGluRA in $\alpha\beta$ KCs whereas we showed the role in γCRE-p KCs. In essence, the studies by Kanellopoulos et al. (2012) revealed the gain-of-function phenotype of DmGluRA, whereas ours demonstrated its loss-of-function phenotype. The DmGluRA signaling may function to set the threshold for memory formation: The high level of the DmGluRA signal may make memory formation tolerant to the weak association, and the low level of the DmGluRA signal enables even a single cycle of training to elicit long-term memory. The formation of long-term memory must be strictly regulated since organisms must select important information from a variety of outside signals. In addition, long-term memory formation consumes energy, and forcing aversive long-term memory formation in starved flies causes premature death (Plaçais and Preat, 2013). However, it is noteworthy that the memory formed on DmGluRA knockdown is defined as long-term memory in the present study, based on three observations: It is inhibited by feeding a protein synthesis inhibitor or expressing the dominant negative CREB, but not by feeding a serotonin blocker that destabilizes anesthesia-resistant memory. Thus, we cannot definitively preclude the possibility that other standards not used in our study may distinguish this memory from the long-term memory formed by a conventional multispaced learning paradigm.

The rdl signaling pathway plays distinct roles in different subtypes of γKCs

Previous studies have suggested that Rdl has an inhibitory effect on both aversive and appetitive memories (X. Liu et al., 2009). These studies primarily focused on the function of Rdl in α/β KCs. Our current investigation examined the roles of Rdl in γKCs, and revealed that Rdl has an inhibitory effect on appetitive memory in γCRE-n KCs, while promoting aversive memory. In contrast, Rdl promotes appetitive memory in γCRE-p KCs, while leaving aversive memory unaffected. Consequently, Rdl exhibits a differential functionality in each type of cell. These observations do not directly contradict previous findings, as γCRE-p KCs are implicated in aversive memory while γCRE-n KCs are associated with appetitive memory, and both subtypes exert mutual inhibition. As a result, these promoting effects would only be discernible when Rdl is knocked down in one of the cell types, as revealed by the current study. However, as this is beyond the scope of our present study, we did not pursue this further.

The roles of DopR2 in olfactory memory

The dopamine receptor DopR2, also known as Damb, reportedly plays a crucial role in the process of forgetting (Berry et al., 2012). Consequently, its inactivation leads to an increase in olfactory memory scores. However, our observations revealed no significant increases in aversive memory scores associated with a *DopR2* null mutant, or the knockdown of DopR2 by two independent RNAi lines. It is imperative to mention that different *DopR2* mutants were used in the two reports, and the efficacy of RNA interference experiments is always subject to the expression levels. Furthermore, the protocol used for scoring aversive memory may vary among laboratories. It is worth noting that Handler et al. (2019) revealed an additional role of DopR2 in backward pairing (2019). However, we did not delve further into this aspect, as our primary focus was on the mGluR signaling pathway.

Subsets of PPL1 DANs serve as gatekeepers for long-term memory

We have shown that even a single round of conditioning is sufficient to induce long-term memory, when vGluT was knocked down either in γ1pedc or in $\gamma2\alpha'1$ DANs. Plaçais et al. (2012) reported that a blockade of these same neurons during the intertrial intervals of spaced conditioning impairs long-term memory formation, and proposed that these neurons play a role in gating long-term memory formation. The same group also found that the Dunce (Dnc) phosphodiesterase, which degrades cAMP, is inhibited in SPN, a pair of serotonergic neurons, during long-term memory formation (Scheunemann et al., 2018). They demonstrated that the transient inhibition of Dnc in SPN is sufficient to induce long-term memory after a single round of conditioning, and the γ1pedc DAN is under the control of SPN, again suggesting the gating role of γ1pedc. The glutamate transmission from the γ1pedc and $\gamma2\alpha'1$ DANs might be involved in this gating function for long-term memory. A recent study using optical voltage recording (Huang et al., 2022) may provide further insight into this issue. The authors indicated that, during the learning process, the induced depression of CS^+-evoked responses in the MBON-γ1pedc $>$ α/β increases the CS^+-evoked responses in PPL1-α3, a known teaching signal for the establishment of long-term memory. Thus, in the absence of DmGluR-mediated inhibition, a single cycle of γ1pedc DAN stimulation may suffice to activate PPL1-α3 by depressing

MBON-γ1pedc $>$ α/β to a degree that is sufficient for the establishment of long-term memory. This could provide a plausible explanation for how changes in the γ1 compartment, responsible for short-term memory, could potentially impact the α3 compartment, which underlies the formation of long-term memory. The aversive long-term memory can also be induced by a single round of conditioning after mild fasting followed by refeeding (Hirano et al., 2013), in which the underlying pathway could be merged at some point with the mGluR signaling.

Possible multiple roles of glutamate co-transmission in DANs

We have demonstrated that the attenuation of mGluR signaling could potentiate both learning and memory consolidation, with even a single cycle of conditioning being sufficient for the occurrence of long-term memory. This finding corroborates the notion that co-transmitters exert a regulatory influence on the memory acquisition process, and particularly on the gating mechanism implicated in the establishment of long-term memory. We have also shown that co-transmitters could function in memory consolidation from a different aspect, since the thermo-genetically evoked PPL1 DANs during consolidation impaired aversive memory, largely because of glutamate signaling. DANs have already been reported to function in consolidation, since multilayered recurrent connections were reported among DANs, KCs, and MBONs (for review, see Adel and Griffith, 2021). In the rodent VTA, some of the dopamine neurons express vesicular glutamate transporter 2, thus making them capable of glutamate co-transmission, and send projections to multiple forebrain regions (Eskenazi et al., 2021). Behavioral analyses have revealed a broad range of roles for dopamine neuron glutamate co-transmission, in responses to psychostimulants, in positive valence and cognitive systems, and in subtle roles in negative valence systems (Eskenazi et al., 2021).

A variety of developmental and physiological conditions may influence the number and activities of vGluT in DANs, which would modify the circuit function and facilitate adaptation according to organisms' experiences and circumstances. Although we only studied the role of co-transmitters in the context of simple associative conditioning here, the co-transmitters may modulate other critical dopamine neuron functions, conveying behavioral states, such as mood, motivation, attention, and arousal, which may collectively reflect phenomena in the real world.

References

Adel M, Griffith LC (2021) The role of dopamine in associative learning in *Drosophila*: an updated unified model. Neurosci Bull 37:831–852.

Aguilar JI, et al. (2017) Neuronal depolarization drives increased dopamine synaptic vesicle loading via VGLUT. Neuron 95:1074–1088.e7.

Akiba M, Sugimoto K, Aoki R, Murakami R, Miyashita T, Hashimoto R, Hiranuma A, Yamauchi J, Ueno T, Morimoto T (2020) Dopamine modulates the optomotor response to unreliable visual stimuli in *Drosophila* melanogaster. Eur J Neurosci 51:822–839.

Ameres SL, Zamore PD (2013) Diversifying microRNA sequence and function. Nat Rev Mol Cell Biol 14:475–488.

Aso Y, Rubin GM (2016) Dopaminergic neurons write and update memories with cell-type-specific rules. Elife 5:e16135.

Aso Y, Siwanowicz I, Bräcker L, Ito K, Kitamoto T, Tanimoto H (2010) Specific dopaminergic neurons for the formation of labile aversive memory. Curr Biol 20:1445–1451.

Aso Y, Herb A, Ogueta M, Siwanowicz I, Templier T, Friedrich AB, Ito K, Scholz H, Tanimoto H (2012) Three dopamine pathways induce aversive odor memories with different stability. PLoS Genet 8:e1002768.

Aso Y, et al. (2014a) Mushroom body output neurons encode valence and guide memory-based action selection in *Drosophila*. Elife 3:e04580.

Aso Y, Hattori D, Yu Y, Johnston RM, Iyer NA, Ngo TT, Dionne H, Abbott L, Axel R, Tanimoto H, Rubin GM (2014b) The neuronal architecture of the mushroom body provides a logic for associative learning. Elife 3: e04577.

Aso Y, Ray RP, Long X, Bushey D, Cichewicz K, Ngo TT, Sharp B, Christoforou C, Hu A, Lemire AL, Tillberg P, Hirsh J, Litwin-Kumar A, Rubin GM (2019) Nitric oxide acts as a cotransmitter in a subset of dopaminergic neurons to diversify memory dynamics. Elife 8:e49257.

Beck CD, Schroeder B, Davis RL (2000) Learning performance of normal and mutant *Drosophila* after repeated conditioning trials with discrete stimuli. J Neurosci 20:2944–2953.

Berry JA, Cervantes-Sandoval I, Nicholas EP, Davis RL (2012) Dopamine is required for learning and forgetting in *Drosophila*. Neuron 74:530–542.

Bolduc FV, Bell K, Cox H, Broadie KS, Tully T (2008) Excess protein synthesis in *Drosophila* Fragile X mutants impairs long-term memory. Nat Neurosci 11:1143–1145.

Brand AH, Perrimon N (1993) Targeted gene expression as a means of altering cell fates and generating dominant phenotypes. Development 118:401–415.

Burke CJ, Huetteroth W, Owald D, Perisse E, Krashes MJ, Das G, Gohl D, Silies M, Certel S, Waddell S (2012) Layered reward signalling through octopamine and dopamine in *Drosophila*. Nature 492:433–437.

Claridge-Chang A, Roorda RD, Vrontou E, Sjulson L, Li H, Hirsh J, Miesenböck G (2009) Writing memories with light-addressable reinforcement circuitry. Cell 139:405–415.

Cognigni P, Felsenberg J, Waddell S (2018) Do the right thing: neural network mechanisms of memory formation, expression and update in *Drosophila*. Curr Opin Neurobiol 49:51–58.

Crittenden JR, Skoulakis EM, Han KA, Kalderon D, Davis RL (1998) Tripartite mushroom body architecture revealed by antigenic markers. Learn Mem 5:38–51.

Deng B, Li Q, Liu X, Cao Y, Li B, Qian Y, Xu R, Mao R, Zhou E, Zhang W, Huang J, Rao Y (2019) Chemoconnectomics: mapping chemical transmission in *Drosophila*. Neuron 101:876–893.e4.

Eskenazi D, Malave L, Mingote S, Yetnikoff L, Ztaou S, Velicu V, Rayport S, Chuhma N (2021) Dopamine Neurons That Cotransmit Glutamate, From Synapses to Circuits to Behavior. Front Neural Circuit 15:665386.

Ffrench-Constant RH, Mortlock DP, Shaffer CD, MacIntyre RJ, Roush RT (1992) Molecular cloning and transformation of cyclodiene resistance in Drosophila: An invertebrate γ-amino-butyric acid subtype A receptor locus. Proc National Acad Sci 89:7849–7849.

Friggi-Grelin F, Coulom H, Meller M, Gomez D, Hirsh J, Birman S (2003) Targeted gene expression in *Drosophila* dopaminergic cells using regulatory sequences from tyrosine hydroxylase. J Neurobiol 54:618–627.

Granger AJ, Wallace ML, Sabatini BL (2017) Multi-transmitter neurons in the mammalian central nervous system. Curr Opin Neurobiol 45:85–91.

Hamada FN, Rosenzweig M, Kang K, Pulver SR, Ghezzi A, Jegla TJ, Garrity PA (2008) An internal thermal sensor controlling temperature preference in *Drosophila*. Nature 454:217–220.

Handler A, Graham TG, Cohn R, Morantte I, Siliciano AF, Zeng J, Li Y, Ruta V (2019) Distinct dopamine receptor pathways underlie the temporal sensitivity of associative learning. Cell 178:60–75.e19.

Hige T (2018) What can tiny mushrooms in fruit flies tell us about learning and memory? Neurosci Res 129:8–16.

Hige T, Aso Y, Modi MN, Rubin GM, Turner GC (2015) Heterosynaptic plasticity underlies aversive olfactory learning in *Drosophila*. Neuron 88:985–998.

Hirano Y, Masuda T, Naganos S, Matsuno M, Ueno K, Miyashita T, Horiuchi J, Saitoe M (2013) Fasting launches CRTC to facilitate long-term memory formation in *Drosophila*. Science 339:443–446.

Honegger KS, Campbell RA, Turner GC (2011) Cellular-resolution population imaging reveals robust sparse coding in the *Drosophila* mushroom body. J Neurosci 31:11772–11785.

Huang C, Luo J, Woo SJ, Roitman L, Li J, Pieribone V, Kannan M, Vasan G, Schnitzer M (2022) Dopamine signals integrate innate and learnt valences to regulate memory dynamics. Research Square.

Huber KM, Gallagher SM, Warren ST, Bear MF (2002) Altered synaptic plasticity in a mouse model of fragile X mental retardation. Proc Natl Acad Sci USA 99:7746–7750.

Jenett A, et al. (2012) A GAL4-driver line resource for *Drosophila* neurobiology. Cell Rep 2:991–1001.

Kanellopoulos AK, Semelidou O, Kotini AG, Anezaki M, Skoulakis EM (2012) Learning and memory deficits consequent to reduction of the fragile X mental retardation protein result from metabotropic glutamate receptor-mediated inhibition of cAMP signaling in *Drosophila*. J Neurosci 32:13111–13124.

Keene AC, Krashes MJ, Leung B, Bernard JA, Waddell S (2006) *Drosophila* dorsal paired medial neurons provide a general mechanism for memory consolidation. Curr Biol 16:1524–1530.

Kim YC, Lee HG, Han KA (2007) D1 dopamine receptor dDA1 is required in the mushroom body neurons for aversive and appetitive learning in *Drosophila*. J Neurosci 27:7640–7647.

Kutlu MG, Tat J, Zachry JE, Calipari ES (2022) Dopamine release at the time of a predicted aversive outcome causally controls the trajectory and expression of conditioned behavior. BioRxiv 2022.04.15.488530.

Lee PT, Lin HW, Chang YH, Fu TF, Dubnau J, Hirsh J, Lee T, Chiang AS (2011) Serotonin-mushroom body circuit modulating the formation of anesthesia-resistant memory in *Drosophila*. Proc Natl Acad Sci USA 108:13794–13799.

Liu C, Plaçais PY, Yamagata N, Pfeiffer BD, Aso Y, Friedrich AB, Siwanowicz I, Rubin GM, Preat T, Tanimoto H (2012) A subset of dopamine neurons signals reward for odour memory in *Drosophila*. Nature 488:512–516.

Liu Q, Tabuchi M, Liu S, Kodama L, Horiuchi W, Daniels J, Chiu L, Baldoni D, Wu MN (2017) Branch-specific plasticity of a bifunctional dopamine circuit encodes protein hunger. Science 356:534–539.

Liu X, Krause WC, Davis RL (2007) GABAA receptor RDL inhibits *Drosophila* olfactory associative learning. Neuron 56:1090–1102.

Liu X, Buchanan ME, Han KA, Davis RL (2009) The GABAA receptor RDL suppresses the conditioned stimulus pathway for olfactory learning. J Neurosci 29:1573–1579.

Luan H, Peabody NC, Vinson CR, White BH (2006) Refined spatial manipulation of neuronal function by combinatorial restriction of transgene expression. Neuron 52:425–436.

Mao Z, Davis RL (2009) Eight different types of dopaminergic neurons innervate the *Drosophila* mushroom body neuropil: anatomical and physiological heterogeneity. Front Neural Circuits 3:5.

McBride SM, Choi CH, Wang Y, Liebelt D, Braunstein E, Ferreiro D, Sehgal A, Siwicki KK, Dockendorff TC, Nguyen HT, McDonald TV, Jongens TA (2005) Pharmacological rescue of synaptic plasticity, courtship behavior, and mushroom body defects in a *Drosophila* model of fragile X syndrome. Neuron 45:753–764.

McGuire SE, Le PT, Osborn AJ, Matsumoto K, Davis RL (2003) Spatiotemporal rescue of memory dysfunction in Drosophila. Science (New York, NY) 302:1765–1768.

Modi MN, Shuai Y, Turner GC (2020) The *Drosophila* mushroom body: from architecture to algorithm in a learning circuit. Annu Rev Neurosci 43:465–484.

Okray Z, Jacob PF, Stern C, Desmond K, Otto N, Vargas-Gutierrez P, Waddell S (2023) Multisensory learning binds modality-specific neurons into a cross-modal memory engram. Nature 617:777–784.

Parmentier ML, Pin JP, Bockaert J, Grau Y (1996) Cloning and functional expression of a *Drosophila* metabotropic glutamate receptor expressed in the embryonic CNS. J Neurosci 16:6687–6694.

Perazzona B, Isabel G, Preat T, Davis RL (2004) The role of cAMP response element-binding protein in *Drosophila* long-term memory. J Neurosci 24:8823–8828.

Plaçais PY, Preat T (2013) To favor survival under food shortage, the brain disables costly memory. Science 339:440–442.

Plaçais PY, Trannoy S, Isabel G, Aso Y, Siwanowicz I, Belliart-Guérin G, Vernier P, Birman S, Tanimoto H, Preat T (2012) Slow oscillations in two pairs of dopaminergic neurons gate long-term memory formation in *Drosophila*. Nat Neurosci 15:592–599.

Qin H, Cressy M, Li W, Coravos JS, Izzi SA, Dubnau J (2012) Gamma Neurons Mediate Dopaminergic Input during Aversive Olfactory Memory Formation in Drosophila. Curr Biol 22:1–7.

Richter JD, Zhao X (2021) The molecular biology of FMRP: new insights into fragile X syndrome. Nat Rev Neurosci 22:209–222.

Riemensperger T, Völler T, Stock P, Buchner E, Fiala A (2005) Punishment prediction by dopaminergic neurons in *Drosophila*. Curr Biol 15:1953–1960.

Scheunemann L, Plaçais PY, Dromard Y, Schwärzel M, Preat T (2018) Dunce phosphodiesterase acts as a checkpoint for *Drosophila* long-term memory in a pair of serotonergic neurons. Neuron 98:350–365.e5.

Schwaerzel M, Monastirioti M, Scholz H, Friggi-Grelin F, Birman S, Heisenberg M (2003) Dopamine and octopamine differentiate between aversive and appetitive olfactory memories in *Drosophila*. J Neurosci 23:10495–10502.

Tanaka NK, Tanimoto H, Ito K (2008) Neuronal assemblies of the *Drosophila* mushroom body. J Comp Neurol 508:711–755.

Tully T, Quinn WG (1985) Classical conditioning and retention in normal and mutant *Drosophila* melanogaster. J Comp Physiol A Neuroethol Sens Neural Behav Physiol 157:263–277.

Tully T, Preat T, Boynton SC, Vecchio MD (1994) Genetic dissection of consolidated memory in *Drosophila*. Cell 79:35–47.

Villar ME, Pavão-Delgado M, Amigo M, Jacob PF, Merabet N, Pinot A, Perry SA, Waddell S, Perisse E (2022) Differential coding of absolute and relative aversive value in the *Drosophila* brain. Curr Biol 32:1–17.

Waddell S (2005) Drosophila memory: dopamine signals punishment? Curr Biol 15:R932–R934.

Xia S, Miyashita T, Fu TF, Lin WY, Wu CL, Pyzocha L, Lin IR, Saitoe M, Tully T, Chiang AS (2005) NMDA receptors mediate olfactory learning and memory in *Drosophila*. Curr Biol 15:603–615.

Yamagata N, Ichinose T, Aso Y, Plaçais PY, Friedrich AB, Sima RJ, Sima RJ, Preat T, Rubin GM, Tanimoto H (2015) Distinct dopamine neurons mediate reward signals for short- and long-term memories. Proc Natl Acad Sci USA 112:578–583.

Yamazaki D, Hiroi M, Abe T, Shimizu K, Minami-Ohtsubo M, Maeyama Y, Horiuchi J, Tabata T (2018) Two parallel pathways assign opposing odor valences during *Drosophila* memory formation. Cell Rep 22:2346–2358.

Yin JC, Wallach JS, Vecchio MD, Wilder EL, Zhou H, Quinn WG, Tully T (1994) Induction of a dominant negative CREB transgene specifically blocks long-term memory in *Drosophila*. Cell 79:49–58.

Zars T, Fischer M, Schulz R, Heisenberg M (2000) Localization of a short-term memory in *Drosophila*. Science 288:672–675.